Host–Guest Chemistry

International Edition: DOI: 10.1002/anie.201501892
German Edition: DOI: 10.1002/ange.201501892

Designed Enclosure Enables Guest Binding Within the 4200 Å^3 Cavity of a Self-Assembled Cube**

*William J. Ramsay, Filip T. Szczypiński, Haim Weissman, Tanya K. Ronson, Maarten M. J. Smulders, Boris Rybtchinski, and Jonathan R. Nitschke**

Abstract: *Metal–organic self-assembly has proven to be of great use in constructing structures of increasing size and intricacy, but the largest assemblies lack the functions associated with the ability to bind guests. Here we demonstrate the self-assembly of two simple organic molecules with Cd^{II} and Pt^{II} into a giant heterometallic supramolecular cube which is capable of binding a variety of mono- and dianionic guests within an enclosed cavity greater than 4200 Å^3. Its structure was established by X-ray crystallography and cryogenic transmission electron microscopy. This cube is the largest discrete abiological assembly that has been observed to bind guests in solution; cavity enclosure and coulombic effects appear to be crucial drivers of host–guest chemistry at this scale. The degree of cavity occupancy, however, appears less important: the largest guest studied, bound the most weakly, occupying only 11 % of the host cavity.*

The spontaneous and precise self-assembly of multiple protein subunits into well-defined, functional superstructures, such as spherical virus capsids[1] and ferritin,[2] inspires the preparation of synthetic analogues.[3] The construction of these nanoscale structures harnesses the self-assembly of rigid organic ligands and metal ions with well-defined coordination spheres,[4] in which the host cavity created by the ligand arrangement allows for diverse applications,[5] such as guest recognition, sensing,[6] and reaction modulation.[7] However, the size and functionality of supramolecular assemblies often run counter to one another: tight, selective binding is achieved by minimizing size,[8] whereas the largest self-assembled structures show no binding properties.[9] Feats such as the encapsulation of ubiquitin[10] require covalent tethering of the guest to the host framework. The development of a method that allows for increasing the size of self-assembled structures whilst maintaining a functional cavity will allow encapsulation chemistry to begin to approach the complexity of biological systems,[11] as larger collections of guests, or larger, more complex discrete guests, may be bound.

The present study builds upon the demonstration that integrative self-sorting is an effective method for assembling subcomponents into a large and complex structure[9a] (**1a**; Figure 1), whereby two different metal ions, Fe^{II} and Pt^{II}, act in concert to define the threefold and fourfold symmetry axes of a cube, respectively. Here we show that by substituting Pd^{II} for Pt^{II} in the self-assembly procedure, a new cube **1b** may be generated, which formed single crystals suitable for X-ray diffraction (see Section 1.2 in the Supporting Information). However, cubes **1a** and **1b** have a porous framework, within which none of a collection of prospective guests[9a] were observed to bind. We thus designed subcomponent **A** (see Section 1.3 in the Supporting Information) to panel[12] the faces of the cubic structure, thereby both enclosing and expanding the cavity (Figure 1).

The reaction between 2-formylpyridine (24 equiv), **A** (24 equiv), cadmium(II) trifluoromethanesulfonate (triflate, 8 equiv), *cis*-bis(benzonitrile)dichloroplatinum(II) (6 equiv), and silver triflate (12 equiv) in acetonitrile produced cage **2** as the uniquely observed product after heating to 50 °C for 8 h (Figure 1; see Section 1.4 in the Supporting Information). When Pd^{II} was used in place of Pt^{II}, or Fe^{II} was used instead of Cd^{II} in the self-assembly procedure, only multiple broad signals were observed in the ^{1}H NMR spectra after 8 h at 50 °C, thus suggesting that a discrete species had not formed. We infer the larger radius of the Cd^{II} ion (109 pm) in comparison to Fe^{II} (75 pm) to be necessary to accommodate the steric demands of the ligand,[13] and that the stronger coordinative pyridine–Pt^{II} bonds[14] may be important in holding the structure together despite minor steric clashes and geometric misalignments. NMR spectroscopic analysis of **2** gave results consistent with the formation of a symmetrical face-capped cubic architecture (Figures S4–S7 in the Supporting Information). The ^{1}H and ^{13}C NMR spectra displayed a single set of signals for the pyridine, anthracene, and phenyl protons of the ligand, which suggests the ligands were rapidly rotating along their axes on the NMR time scale. A single

[*] W. J. Ramsay, F. T. Szczypiński, Dr. T. K. Ronson, Prof. J. R. Nitschke
University of Cambridge, Department of Chemistry
Lensfield Road, Cambridge, CB2 1EW (UK)
E-mail: jrn34@cam.ac.uk
Homepage: http://www-jrn.ch.cam.ac.uk/
Dr. H. Weissman, Prof. B. Rybtchinski
Weizmann Institute of Science, Department of Organic Chemistry
Rehovot, 76100 (Israel)
Dr. M. M. J. Smulders
Wageningen University, Laboratory of Organic Chemistry
P.O. Box 8026, 6700EG Wageningen (The Netherlands)

[**] This work was supported by the Marie Curie Academic-Industrial Initial Training Network on Dynamic Molecular Nanostructures (DYNAMOL; W.J.R.) and the Engineering and Physical Sciences Research Council (EPSRC). B.R. and H.W. acknowledge support from the Gerhardt M. J. Schmidt Minerva Centre of Supramolecular Architectures and the Helen and Martin Kimmel Centre for Molecular Design. The TEM studies were conducted at the Irving and Cherna Moskowitz Centre for Nano and Bio-Nano Imaging (Weizmann Institute). M.M.J.S. acknowledges support from The Netherlands Organization for Scientific Research. We thank Diamond Light Source (UK) for synchrotron beamtime on I19 (MT7569 and MT8464).

Supporting information for this article is available on the WWW under http://dx.doi.org/10.1002/anie.201501892.

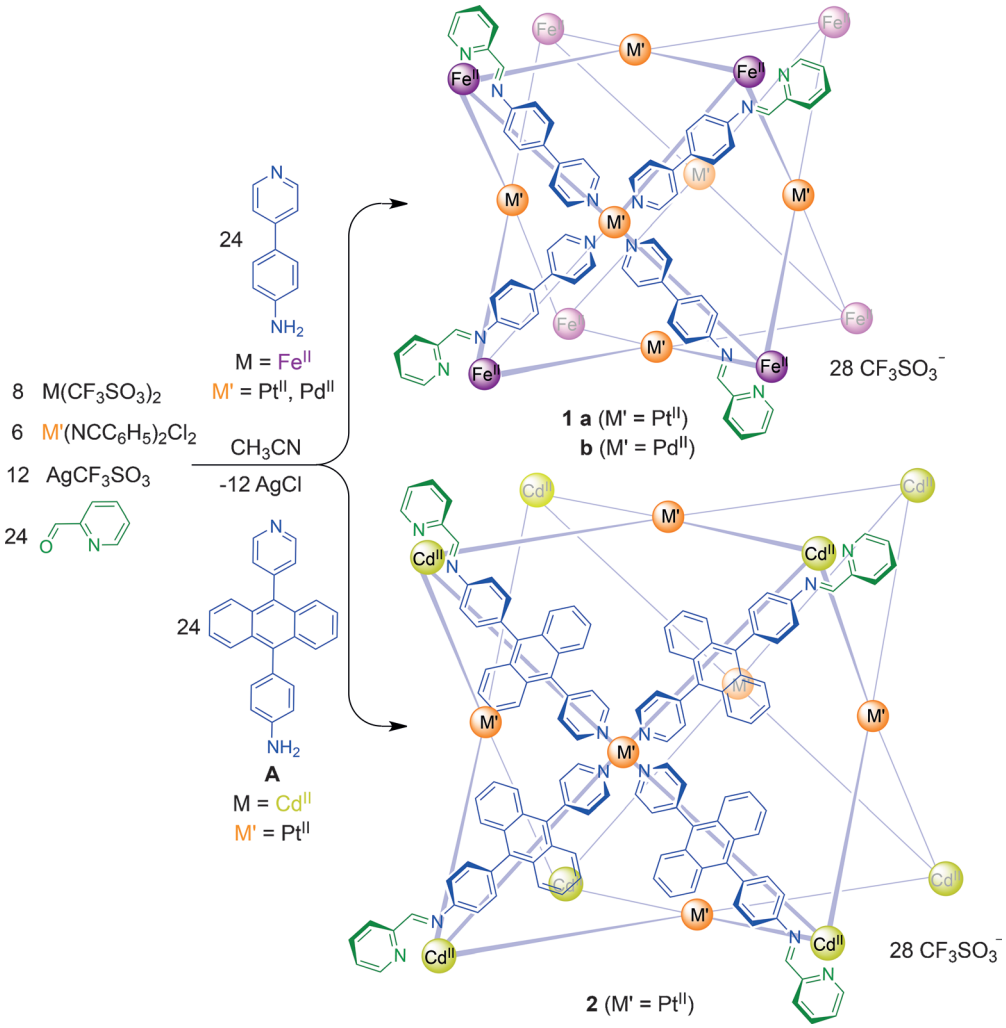

Figure 1. The one-pot synthetic procedure for cubes **1a** and **b** starting from free subcomponents and metal ions (top) was adapted to prepare cube **2** from subcomponent **A**; only one cube face is shown in each case for clarity.

diffusion coefficient (log(D)) of −9.48 was observed for **2** in the DOSY spectrum (Figure S8). High-resolution electrospray ionization mass spectrometry (HRMS-ESI) produced results consistent with fragments of the proposed structure of **2** (Figure S9), but no signals were observed at the *m*/*z* value of the parent ion; we infer that the high charge and large size of the structure resulted in its fragmentation in the gas phase.[15]

Single-crystal X-ray diffraction at Diamond Light Source[16] revealed the solid-state structures of **1b** and **2**. The approximately *O*-symmetric solid-state structure of **1b** (Figure 2a,c) is consistent with the high-symmetry NMR spectra recorded in solution. Although X-ray analysis identified eight BF_4^- ions occupying the cavity of **1b** (Figure 2a), no evidence of encapsulation was observed in solution by ^{19}F NMR spectroscopy. The eight tris(pyridylimine)iron(II) vertices in **1b** all have the same Δ or Λ stereochemistry; both enantiomers are present in the crystal lattice. Although the eight tris(pyridylimine)cadmium(II) vertices in **2** also have facial stereochemistry, X-ray analysis identified four metal centers on one face to have Λ handedness, with four Δ metal centers opposite, thus giving the cube approximate C_s point symmetry, which has not previously been observed for M_8L_6 structures[17] (Figure 2b,d). As the observed NMR spectra of **2** in solution indicated higher symmetry, we posit that the solid-state arrangement of **2** resulted from maximization of C–H···π interactions between neighboring anthracenes around the corners, thereby rendering the C_s diastereomer the most energetically favorable conformation in the solid state.

In both **1b** and **2**, the cube faces consist of six square-planar Pd^{II} and Pt^{II} metal ions, respectively, coordinated by the pyridine moieties. The four pyridyl rings around the central square-planar metal ion are sterically constrained to lie orthogonally to the cube face. In the case of **2**, the anthracenyl group of **A** is in turn constrained to orthogonality with the pyridyl ring, thus leading it to lie roughly parallel to its cube face. This parallel orientation provides enclosure; longer analogues of **A** could be similarly designed to provide access to yet larger enclosed architectures.

The diagonal distance across the cube from the outermost hydrogen atoms of the farthest-spaced ligands is 3.5 nm in **1b**, and 5.0 nm in **2**, which rivals the size of the largest structurally characterized synthetic metal–organic structures.[3a,18] Importantly, **2** encloses a cavity of 4225 $Å^3$ (see Section 1.4.1 in the Supporting Information), which dynamic motion in solution might further increase to up to 7000 $Å^3$: the cavity size for **2** in which the anthracenyl groups are modeled to lie strictly parallel to the cube faces. In the crystal, some of these groups protrude slightly into the cavity, as a result of crystal-packing effects, thus reducing the volume available for guest binding.

Cube **2** has large faces that can come together in aqueous media, thereby leading to the formation of superstructures.[19] We employed cryogenic transmission electron microscopy (cryo-TEM) imaging to visualize directly the structure of **2** in a 1:1 water/acetonitrile solution (3×10^{-6} M; Figure 3). The cryo-TEM images displayed lamellar structures consistent with the formation of aggregates of **2**. When these structures

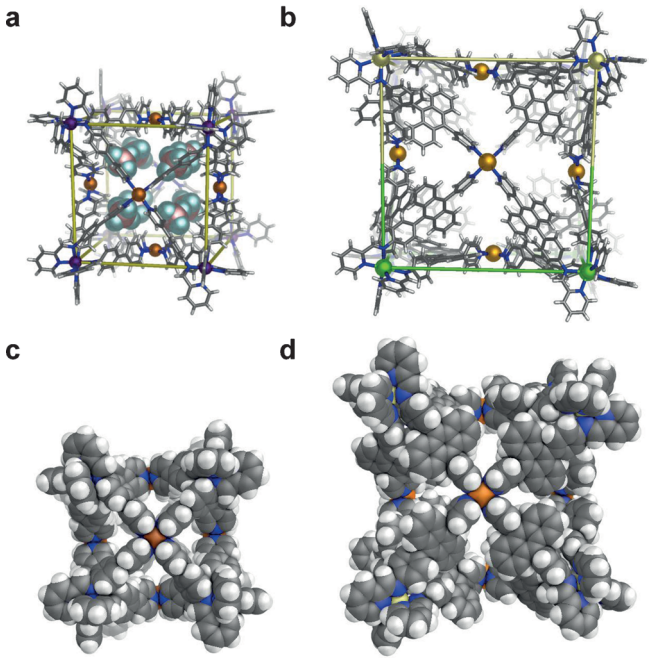

Figure 2. Framework representation of the X-ray crystal structure of a) [**1 b**][BF_4]$_{28}$, where the 8 BF_4^- anions occupying the cavity are shown in space-filling representation, and b) **2**, where Cd^{II} centers of Δ handedness are shown in green, and Cd^{II} centers of opposite Λ handedness are shown in light yellow. The space-filling representation of c) [**1 b**][BF_4]$_{28}$ shows the pores at the edges of the cube, which are effectively closed off by the anthracene paneling in **2** (d). Color scheme: C gray, N blue, Fe purple, H white, Pt light orange, Pd dark orange, F light blue, B pink. Disordered, non-encapsulated anions and solvent molecules are omitted for clarity. The edges of both cubic frameworks are highlighted by lines. All structures are depicted at the same scale.

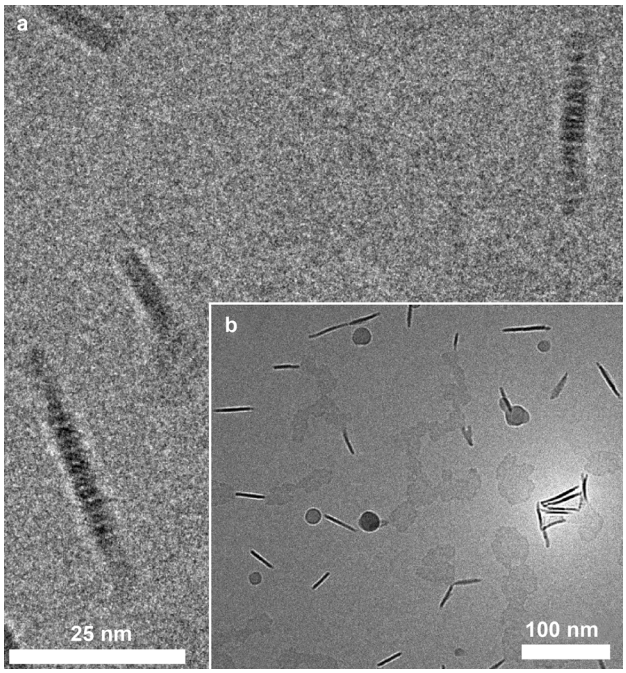

Figure 3. Cryo-TEM images of **2** in a 1:1 water/acetonitrile solution (3×10^{-6} M) a) Higher magnification of the stick-like structures in (b) reveals segmented features. b) Monomolecular lamellar structures are observed in different orientations relative to the optical axis. The stick-like structures (the lamella) as viewed from the side (lamella cross-sections that are parallel to optical axis); round features are due to ice contamination.

are perpendicular to the optical axis, lower contrast platelets are observed due to a thinner optical pathway; when parallel to the optical axis, the lamellae exhibit high-contrast cross-sections (20 to 200 nm long, Figure 3b and Figure S11). The thickness of the lamellae cross-sections is 3.1 ± 0.2 nm, and their straightness is indicative of rigidity. The segmented nature of the cross-sections is revealed at high magnification (Figure 3a and Figure S12). The periodicity of the segments is 1.9 nm, which corresponds to a cube–cube spacing of 3.8 nm; it is consistent with the cubes (3.4 nm in length) stacking through their parallel faces. Hierarchical organization of individual **2** units into the ordered rigid monolayer, as observed by cryo-TEM, appears to result from an energetic balance between ionic and hydrophobic interactions. Although robust, covalently linked 2D structures on this length scale have been imaged on surfaces,[20] we are not aware of other cases where hierarchical, noncovalently linked assemblies having porous structures have been directly observed without the need for a surface support.[21]

The guest-binding properties of **2** were investigated by screening the same neutral and anionic guests explored previously with **1 a**[9a] and **1 b**. Although no neutral guests were found to undergo complexation, several large, anionic species were observed to bind inside the cavity of **2**, including hexamolybdate ($Mo_6O_{19}^{2-}$), dodecafluoro-*closo*-dodecaborate ($B_{12}F_{12}^{2-}$), tetraphenylborate (BPh_4^-), carborane ($CB_{11}H_{12}^-$), and tetrakis(pentafluorophenyl)borate ($B(C_6F_5)_4^-$; see Sections 3.1–3.5, respectively, in the Supporting Information). In all the studies, the binding processes were followed by ^{1}H NMR titrations in [D_3]acetonitrile, whereby the pyridine protons closest to the Pt^{II} centers on the faces of **2** (H^1) were observed to shift upfield upon saturation of the solution with a guest, thus indicating fast exchange on the NMR time scale; the imine peak of **2** also underwent spectral shifts consistent with guest binding. Such shifts were not observed during host–guest investigations with **1 a** or **1 b**, and we infer they were caused by binding of the guest to the cavity of **2**. Downfield chemical shifts in the ^{19}F NMR spectra of the fluorinated species $B_{12}F_{12}^{2-}$ and $B(C_6F_5)_4^-$ were observed (Figures S18 and S27, respectively) in the presence of **2**, consistent with their binding. NOESY correlations between BPh_4^- and the Pt^{II}-bound pyridine protons from **2** (H^1 and H^2) were observed (Figure S21), which suggested a Coulombic attraction of the negatively charged guest to the center of the faces of the host; the DOSY spectrum of the host–guest complex also revealed a slower diffusion coefficient for BPh_4^- when compared to free BPh_4^- in solution (Figure S22). Job's plots by UV/Vis spectroscopy identified the stoichiometry of binding to be 1:1 in all cases, and the titration data were, therefore, fitted to 1:1 binding isotherms (see Section 3 in the Supporting Information); the low solubility of the host–guest complexes required the stoichiometry experiments to be

Table 1: Binding constants (K_a, M^{-1}) of selected guests with cubic host **2** (determined at 298 K in acetonitrile).

Guest	Host **1a,b**	**2**	occupancy [%][b]
$TBA_2Mo_6O_{19}$[a]		$2.9 \pm 0.4 \times 10^3$	6.4
$K_2B_{12}F_{12}$		$2.2 \pm 0.1 \times 10^3$	6.1
$TBABPh_4$[a]	no binding	$5.22 \pm 0.07 \times 10^2$	8.8
$CsCB_{11}H_{12}$		$2.05 \pm 0.08 \times 10^2$	5.2
$TBA(B(C_6F_5)_4)$[a]		$4 \pm 1 \times 10^1$	11.1

[a] TBA = tetra-*n*-butylammonium. [b] See Section 1.4.2 in the Supporting Information.

performed at UV/Vis concentrations. The association constants are summarized in Table 1.

The observation that the dianions ($Mo_6O_{19}^{2-}$ and $B_{12}F_{12}^{2-}$) bound an order of magnitude more strongly than the monoanions (BPh_4^-, $CB_{11}H_{12}^-$, and $B(C_6F_5)_4^-$) is consistent with attractive electrostatic forces constituting a major driving force for encapsulation between the 28 + charged host and anionic guests. A larger guest, $Mo_6O_{19}^{2-}$, was also observed to bind more strongly than a smaller guest, $B_{12}F_{12}^{2-}$. This observation is consistent with higher occupancy leading to better binding, despite the low occupancy factors observed with all anions (Table 1); we infer at least part of the remaining cavity volume to be occupied by solvent molecules.[22] The interaction of the more electron-rich π clouds of BPh_4^- also appear to contribute to its binding with the host's electron-deficient framework,[23] as weaker binding affinity was observed with the less π-basic $B(C_6F_5)_4^-$.

The results presented herein illustrate how the rational design of subcomponents in tandem with self-assembly processes can provide a means to generate large, hollow architectures, while maintaining a sufficiently closed cavity to allow for host–guest interactions. Our study offers a clear approach to the generation of even larger structures with well-defined porosities,[24] at the same time offering new guidance as to the factors important for the observation of guest binding.

Keywords: electron microscopy · host–guest chemistry · integrative self-sorting · metal–organic cages · supramolecular chemistry

How to cite: *Angew. Chem. Int. Ed.* **2015**, *54*, 5636–5640
Angew. Chem. **2015**, *127*, 5728–5732

[1] S. Casjens, *Virus Structure and Assembly*, Jones and Bartlett, Sudbury, **1985**.
[2] E. C. Theil, *Annu. Rev. Biochem.* **1987**, *56*, 289–315.
[3] a) Q.-F. Sun, J. Iwasa, D. Ogawa, Y. Ishido, S. Sato, T. Ozeki, Y. Sei, K. Yamaguchi, M. Fujita, *Science* **2010**, *328*, 1144–1147; b) M. D. Ward, *Chem. Commun.* **2009**, 4487–4499; c) R. Chakrabarty, P. S. Mukherjee, P. J. Stang, *Chem. Rev.* **2011**, *111*, 6810–6918; d) D. Fiedler, D. H. Leung, R. G. Bergman, K. N. Raymond, *Acc. Chem. Res.* **2005**, *38*, 349–358; e) P. Ballester, *Chem. Soc. Rev.* **2010**, *39*, 3810–3830; f) G. M. Whitesides, B. Grzybowski, *Science* **2002**, *295*, 2418–2421; g) T. K. Ronson, S. Zarra, S. P. Black, J. R. Nitschke, *Chem. Commun.* **2013**, *49*, 2476–2490.
[4] a) B. Olenyuk, J. A. Whiteford, A. Fechtenkotter, P. J. Stang, *Nature* **1999**, *398*, 796–799; b) T. Heinz, D. M. Rudkevich, J. Rebek, *Nature* **1998**, *394*, 764–766; c) M. Fujita, D. Oguro, M. Miyazawa, H. Oka, K. Yamaguchi, K. Ogura, *Nature* **1995**, *378*, 469–471; d) D. L. Caulder, C. Brückner, R. E. Powers, S. König, T. N. Parac, J. A. Leary, K. N. Raymond, *J. Am. Chem. Soc.* **2001**, *123*, 8923–8938; e) T. K. Ronson, J. Fisher, L. P. Harding, P. J. Rizkallah, J. E. Warren, M. J. Hardie, *Nat. Chem.* **2009**, *1*, 212–216; f) M. Albrecht, Y. Shang, T. Rhyssen, J. Stubenrauch, H. D. F. Winkler, C. A. Schalley, *Eur. J. Org. Chem.* **2012**, *2012*, 2422–2427; g) T. Weilandt, U. Kiehne, J. Bunzen, G. Schnakenburg, A. Lützen, *Chem. Eur. J.* **2010**, *16*, 2418–2426; h) J. Dömer, J. C. Slootweg, F. Hupka, K. Lammertsma, F. E. Hahn, *Angew. Chem. Int. Ed.* **2010**, *49*, 6430–6433; *Angew. Chem.* **2010**, *122*, 6575–6578.
[5] a) J. M. Rivera, T. Martín, J. Rebek, *Science* **1998**, *279*, 1021–1023; b) S. Mirtschin, A. Slabon-Turski, R. Scopelliti, A. H. Velders, K. Severin, *J. Am. Chem. Soc.* **2010**, *132*, 14004–14005; c) Y. Li, A. H. Flood, *J. Am. Chem. Soc.* **2008**, *130*, 12111–12122; d) D. Ray, J. T. Foy, R. P. Hughes, I. Aprahamian, *Nat. Chem.* **2012**, *4*, 757–762; e) G. Zhang, O. Presly, F. White, I. M. Oppel, M. Mastalerz, *Angew. Chem. Int. Ed.* **2014**, *53*, 5126–5130; *Angew. Chem.* **2014**, *126*, 5226–5230.
[6] a) R. Custelcean, P. V. Bonnesen, N. C. Duncan, X. Zhang, L. A. Watson, G. Van Berkel, W. B. Parson, B. P. Hay, *J. Am. Chem. Soc.* **2012**, *134*, 8525–8534; b) S. K. Samanta, M. Schmittel, *Org. Biomol. Chem.* **2013**, *11*, 3108–3115; c) R. Frantz, C. S. Grange, N. K. Al-Rasbi, M. D. Ward, J. Lacour, *Chem. Commun.* **2007**, 1459–1461; d) S. Liu, A. D. Shukla, S. Gadde, B. D. Wagner, A. E. Kaifer, L. Isaacs, *Angew. Chem. Int. Ed.* **2008**, *47*, 2657–2660; *Angew. Chem.* **2008**, *120*, 2697–2700; e) M. M. Tsotsalas, K. Kopka, G. Luppi, S. Wagner, M. P. Law, M. Schäfers, L. De Cola, *ACS Nano* **2010**, *4*, 342–348; f) G. H. Clever, S. Tashiro, M. Shionoya, *Angew. Chem. Int. Ed.* **2009**, *48*, 7010–7012; *Angew. Chem.* **2009**, *121*, 7144–7146; g) S. Löffler, J. Lübben, L. Krause, D. Stalke, B. Dittrich, G. H. Clever, *J. Am. Chem. Soc.* **2015**, *137*, 1060–1063.
[7] a) M. Yoshizawa, J. K. Klosterman, M. Fujita, *Angew. Chem. Int. Ed.* **2009**, *48*, 3418–3438; *Angew. Chem.* **2009**, *121*, 3470–3490; b) A. G. Salles, S. Zarra, R. M. Turner, J. R. Nitschke, *J. Am. Chem. Soc.* **2013**, *135*, 19143–19146; c) Q. Zhang, K. Tiefenbacher, *Nat. Chem.* **2015**, *7*, 197–202.
[8] a) Q.-Q. Wang, V. W. Day, K. Bowman-James, *Angew. Chem. Int. Ed.* **2012**, *51*, 2119–2123; *Angew. Chem.* **2012**, *124*, 2161–2165; b) Y. Ahn, Y. Jang, N. Selvapalam, G. Yun, K. Kim, *Angew. Chem. Int. Ed.* **2013**, *52*, 3140–3144; *Angew. Chem.* **2013**, *125*, 3222–3226.
[9] a) M. M. J. Smulders, A. Jiménez, J. R. Nitschke, *Angew. Chem. Int. Ed.* **2012**, *51*, 6681–6685; *Angew. Chem.* **2012**, *124*, 6785–6789; b) B. Olenyuk, M. D. Levin, J. A. Whiteford, J. E. Shield, P. J. Stang, *J. Am. Chem. Soc.* **1999**, *121*, 10434–10435.
[10] D. Fujita, K. Suzuki, S. Sato, M. Yagi-Utsumi, Y. Yamaguchi, N. Mizuno, T. Kumasaka, M. Takata, M. Noda, S. Uchiyama, K. Kato, M. Fujita, *Nat. Commun.* **2012**, *3*, 1093.
[11] P. A. de Silva, N. H. Q. Gunaratne, C. P. McCoy, *Nature* **1993**, *364*, 42–44.
[12] N. Kishi, M. Akita, M. Yoshizawa, *Angew. Chem. Int. Ed.* **2014**, *53*, 3604–3607; *Angew. Chem.* **2014**, *126*, 3678–3681.
[13] a) W. Meng, T. K. Ronson, J. K. Clegg, J. R. Nitschke, *Angew. Chem. Int. Ed.* **2013**, *52*, 1017–1021; *Angew. Chem.* **2013**, *125*, 1051–1055; b) R. D. Shannon, *Acta Crystallogr. Sect. A* **1976**, *32*, 751–767.
[14] D. Fujita, A. Takahashi, S. Sato, M. Fujita, *J. Am. Chem. Soc.* **2011**, *133*, 13317–13319.
[15] C. A. Schalley, *Mass Spectrom. Rev.* **2001**, *20*, 253–309.
[16] a) H. Nowell, S. A. Barnett, K. E. Christensen, S. J. Teat, D. R. Allan, *J. Synchrotron Radiat.* **2012**, *19*, 435–441;

b) CCDC 1041134 – 1041135 contain the supplementary crystallographic data for this paper. These data can be obtained free of charge from The Cambridge Crystallographic Data Centre via www.ccdc.cam.ac.uk/data_request/cif.

[17] a) W. Meng, B. Breiner, K. Rissanen, J. D. Thoburn, J. K. Clegg, J. R. Nitschke, *Angew. Chem. Int. Ed.* **2011**, *50*, 3479 – 3483; *Angew. Chem.* **2011**, *123*, 3541 – 3545; b) W. J. Ramsay, T. K. Ronson, J. K. Clegg, J. R. Nitschke, *Angew. Chem. Int. Ed.* **2013**, *52*, 13439 – 13443; *Angew. Chem.* **2013**, *125*, 13681 – 13685; c) H.-B. Wu, Q.-M. Wang, *Angew. Chem. Int. Ed.* **2009**, *48*, 7343 – 7345; *Angew. Chem.* **2009**, *121*, 7479 – 7481.

[18] a) R. A. Bilbeisi, T. K. Ronson, J. R. Nitschke, *Angew. Chem. Int. Ed.* **2013**, *52*, 9027 – 9030; *Angew. Chem.* **2013**, *125*, 9197 – 9200; b) S. Pasquale, S. Sattin, E. C. Escudero-Adán, M. Martínez-Belmonte, J. de Mendoza, *Nat. Commun.* **2012**, *3*, 785.

[19] a) H. Weissman, B. Rybtchinski, *Curr. Opin. Colloid Interface Sci.* **2012**, *17*, 330 – 342; b) L. Wasserthal, B. Schade, K. Ludwig, C. Böttcher, A. Hirsch, *Chem. Eur. J.* **2014**, *20*, 5961 – 5966.

[20] A. Saywell, J. K. Sprafke, L. J. Esdaile, A. J. Britton, A. Rienzo, H. L. Anderson, J. N. O'Shea, P. H. Beton, *Angew. Chem. Int. Ed.* **2010**, *49*, 9136 – 9139; *Angew. Chem.* **2010**, *122*, 9322 – 9325.

[21] A. G. Slater, P. H. Beton, N. R. Champness, *Chem. Sci.* **2011**, *2*, 1440 – 1448.

[22] S. Mecozzi, J. J. Rebek, *Chem. Eur. J.* **1998**, *4*, 1016 – 1022.

[23] H. T. Chifotides, I. D. Giles, K. R. Dunbar, *J. Am. Chem. Soc.* **2013**, *135*, 3039 – 3055.

[24] T. Hasell, H. Zhang, A. I. Cooper, *Adv. Mater.* **2012**, *24*, 5732 – 5737.

Received: February 27, 2015
Published online: April 14, 2015

